Inorganica Chimica Acta 432 (2015) 89–95

Contents lists available at ScienceDirect

Inorganica Chimica Acta

journal homepage: www.elsevier.com/locate/ica

Syntheses, hydrogen-bonded assembly structures, and spin crossover properties of $[Fe^{III}(Him)_2(n\text{-}MeOhapen)]PF_6$ (Him = imidazole and n-MeOhapen = *N,N′*-bis(n-methoxy-2-oxyacetophenylidene) ethylenediamine); *n* = 4, 5, 6)

Takeshi Fujinami [a,*], Mizuki Ikeda [a], Masataka Koike [a], Naohide Matsumoto [a], Tomohiro Oishi [b], Yukinari Sunatsuki [c]

[a] Department of Chemistry, Faculty of Science, Kumamoto University, Kurokami 2-39-1, Kumamoto 860-8555, Japan
[b] Technical Division, Faculty of Engineering, Kumamoto University, Kurokami 2-39-1, Kumamoto 860-8555, Japan
[c] Department of Chemistry, Faculty of Science, Okayama University, Tsushima-naka 1-1, Okayama 700-8530, Japan

ARTICLE INFO

Article history:
Received 30 October 2014
Received in revised form 9 January 2015
Accepted 22 March 2015
Available online 3 April 2015

Keywords:
Iron(III) complex
Spin equilibrium
Imidazole
N_2O_2 Schiff-base ligand
Hydrogen bonds
Assembly structures

ABSTRACT

Three iron(III) complexes, $[Fe^{III}(Him)_2(n\text{-}MeOhapen)]PF_6$ (**1**: *n* = 4, **2**: *n* = 5, **3**: *n* = 6), where Him = imidazole and n-MeOhapen = *N,N′*-bis(n-methoxy-2-oxyacetophenylidene)ethylenediamine, were synthesized. Each Fe^{III} ion was coordinated by N_4O_2 donor atoms of equatorial n-MeOhapen and two axial Him. The saturated FeC_2N_2 chelate ring involving the ethylenediamine moiety adopted a gauche conformation and the two phenylidene planes of $[Fe^{III}(Him)_2(n\text{-}MeOhapen)]^+$ were oriented opposite to the FeO_2N_2 coordination plane. Two adjacent $[Fe^{III}(Him)_2(4\text{-}MeOhapen)]^+$ cations in **1** were connected via PF_6^- ions by hydrogen bonds between the imidazole group and PF_6^- to give a one-dimensional chain. Two adjacent cations in **2** were connected via hydrogen bonds between the phenylidene oxygen and imidazole atoms to form a cyclic dimer structure. Two EtOH molecules were involved in a hydrogen-bonded cyclic dimer structure in **3**. Compounds **1** and **2** showed spin crossover behavior, but **3** showed incomplete spin crossover.

© 2015 Elsevier B.V. All rights reserved.

1. Introduction

Spin crossover (SCO) is a representative phenomenon of bistability in the electronic structure of metal complexes. SCO complexes show inter-conversion between the high-spin (HS) and low-spin (LS) states upon external physical perturbations such as temperature, pressure, and light irradiation [1]. Steepness, multi-step, and hysteresis in SCO profiles can be induced by intermolecular cooperative effects [1].

Among metal complexes that exhibit SCO, SCO Fe^{III} complexes with a d^5 electronic configuration generally exhibit a gradual spin equilibrium [2] and show no thermal hysteresis with the exception of a few complexes [3]. On the other hand, some SCO Fe^{II} complexes with a d^6 electronic configuration show steep spin transitions that exhibit thermal hysteresis [1]. Fe^{II} and Fe^{III} complexes with a tetradentate planar ligand and two monodentate axial ligands exhibit SCO [2–5], and the SCO complexes with bidentate or tridentate ligands are major groups in SCO studies [1,6]. The Fe^{II} or Fe^{III} sites in some heme proteins exhibit SCO properties [7], and iron porphyrin derivatives have been studied as model compounds [8]. As synthetic, yet simple model compounds, Nishida first reported a family of Fe^{III} complexes with N_2O_2 salen-type ligands at the equatorial plane and two monodentate ligands (monodentate ligands such as pyridine and imidazole derivatives) at the axial sites $[Fe^{III}(X)_2(salen\text{-}type)]BPh_4$ [9] and demonstrated that the ligand field of $[Fe^{III}(X)_2(salen\text{-}type)]^+$ is close to the SCO point and that some of them exhibit SCO. Subsequently, Matsumoto [10], Murray [11], and Real [12] reported SCO Fe^{III} complexes with analogous N_2O_2 Schiff-base ligands and revealed the relevant factors to determine the SCO properties. Especially, Murray [11] pointed out that the conformation of the two phenylidene planes of $[Fe^{III}(X)_2(salen\text{-}type)]^+$ with a one side opened salen-type ligand is related to "whether or not SCO occurs". The favored conformation is not always achieved for $[Fe^{III}(X)_2(salen\text{-}type)]^+$, and even if SCO was observed, steep SCO with hysteresis was not merely observed.

* Corresponding author. Tel./fax: +81 96 342 3385.
E-mail address: tfujinami@sci.kumamoto-u.ac.jp (T. Fujinami).

http://dx.doi.org/10.1016/j.ica.2015.03.034
0020-1693/© 2015 Elsevier B.V. All rights reserved.

In previous papers, we revealed that "hapen-type" ligands in $[Fe^{III}(X)_2(hapen\text{-}type)]^+$ (Scheme 1) can give the suitable conformation due to the steric hindrance between the methyl group on the phenylidene moiety and five-membered chelate ring [10d]. Furthermore, an imidazole group as the axial ligand X in $[Fe^{III}(X)_2(hapen\text{-}type)]^+$ can form intermolecular hydrogen-bonds to generate an assembly structure that may lead to cooperative effects and modify the SCO profile. One of these complexes, $[Fe^{III}(Him)_2(hapen)]AsF_6$, showed steep SCO with thermal hysteresis [4]. Some of SCO properties, such as steep, multi-step spin transitions, hysteresis, and light-induced excited spin-state trapping (LIESST), depend on the intermolecular hydrogen-bonds among the SCO molecules [13]. In this study, three Fe^{III} complexes $[Fe^{III}(Him)_2(n\text{-}MeOhapen)]PF_6$ (**1**: $n = 4$, **2**: $n = 5$, **3**: $n = 6$) with three isomers of the new "hapen-type" ligand (n-MeOhapen) were synthesized. In addition to the favorable conformation of the "hapen-type" ligand and intermolecular hydrogen bond by imidazole group, the methoxy group may modify the intermolecular interactions. From the above described three points; (1) the molecular conformation of the two phenylidene planes (2) intermolecular interactions by hydrogen bonds by with the imidazole moiety, and (3) modification of the assembly structure by the methoxy group, we have synthesized three Fe^{III} complexes $[Fe^{III}(Him)_2(n\text{-}MeOhapen)]PF_6$ (**1**: $n = 4$, **2**: $n = 5$, **3**: $n = 6$)(Scheme 1), and reported here the syntheses, structures, and SCO properties.

2. Experimental

2.1. General

All reagents and solvents used in the syntheses are commercially available from Tokyo Kasei Co., Ltd., Tokyo, Japan and Wako Pure Chemical Industries, Ltd., Osaka, Japan, and were used without further purification. All of the synthetic procedures were performed in air.

2.2. Preparation of materials

2.2.1. Preparations of tetradentate ligand H_2(n-MeOhapen) solvents and precursor iron(III) complex $[Fe^{III}Cl(n\text{-}MeOhapen)]$ solvents

2.2.1.1. H_2(4-MeOhapen). To a solution of 4-methoxy-2-hydroxyacetophenone (0.05 mol, 8.31 g) in 50 mL of ethanol, a solution of ethylenediamine (0.025 mol, 1.51 g) in 50 mL of ethanol was added, and the mixture was stirred for 30 min on a hot plate at 60 °C. The resulting yellow crystalline material was collected by suction filtration, washed with a small amount of ethanol, and dried in vacuo. Yield: 7.30 g (82%). *Anal.* Calc. for H_2(4-MeOhapen) ($C_{20}H_{24}N_2O_4$): C, 67.40; H, 6.79; N, 7.86. mp = 254 °C. Found: C, 67.09; H, 6.85; N, 7.86%. IR: $\nu_{C=N}$ 1583 cm^{-1}. ^1H NMR ($CDCl_3$, 400 MHz, ppm): δ 7.38–7.36 (1H, d), 6.36 (1H, d), 6.31–6.28 (1H, q), 3.92 (2H, s), 3.79 (3H, s), 2.34 (3H, s). Here, s, d, t, and q indicate singlet, doublet, triplet, and quartet, respectively.

2.2.1.2. H_2(5-MeOhapen). The tetradentate Schiff-base ligand H_2(5-MeOhapen) was prepared by a similar method to that used in the preparation of H_2(4-MeOhapen), using 5-methoxy-2-hydroxyacetophenone instead of 4-methoxy-2-hydroxyacetophenone. A yellow crystalline material was obtained as the product. Yield: 6.22 g (87%). *Anal.* Calc. for H_2(5-MeOhapen) ($C_{20}H_{24}N_2O_4$): C, 67.40; H, 6.79; N, 7.86. Found: C, 67.19; H, 6.81; N, 7.77%. mp = 251 °C. IR: $\nu_{C=N}$ 1614 cm^{-1}. ^1H NMR ($CDCl_3$, 400 MHz, ppm): δ 7.04 (1H, d), 6.93–6.90 (1H, q), 6.87–6.84 (1H, d) 3.97 (2H, s), 3.77 (3H, s), 2.35 (3H, s).

2.2.1.3. H_2(6-MeOhapen)·0.25EtOH. The tetradentate Schiff-base ligand H_2(6-MeOhapen)·0.25EtOH was prepared by a similar method to that used in the preparation of H_2(4-MeOhapen), using 6-methoxy-2-hydroxyacetophenone instead of 4-methoxy-2-hydroxyacetophenone. A yellow crystalline material was obtained. Yield: 6.16 g (67%). *Anal.* Calc. for H_2(6-MeOhapen)·0.25EtOH ($C_{20}H_{24}N_2O_4$·0.25EtOH): C, 66.91; H, 6.99; N, 7.61. Found: C, 66.67; H, 6.91; N, 7.72%. mp = 197 °C. IR: $\nu_{C=N}$ 1600 cm^{-1}. ^1H NMR ($CDCl_3$, 400 MHz, ppm): δ 7.17–7.13 (1H, t), 6.54–6.52 (1H, q), 6.28–6.26 (1H, q), 3.91 (2H, s), 3.81 (3H, s), 2.47 (3H, s).

*2.2.1.4. $[FeCl(4\text{-}MeOhapen)]\cdot H_2O$ **1′**.* The precursor iron(III) complex $[Fe^{III}Cl(4\text{-}MeOhapen)]\cdot H_2O$ was prepared according to the method applied for $[Fe^{III}Cl(salen)]$. To a solution of H_2(4-MeOhapen) (0.01 mol, 3.56 g) in 150 mL of methanol, anhydrous $Fe^{III}Cl_3$ (0.01 mol, 1.62 g) was added, and the mixture was stirred for 30 min on hot-plate at 65 °C. To the hot solution, a solution of triethylamine (0.02 mol, 2.02 g) in 10 mL of methanol was added dropwise. The resulting black crystals were collected by suction filtration, washed with a small amount of diethylether, and dried in vacuo. Yield: 4.18 g (93%). *Anal.* Calc. for $[FeCl(4\text{-}MeOhapen)]\cdot H_2O$ ($C_{20}H_{24}N_2O_4FeCl\cdot H_2O$): C, 51.80; H, 5.22; N, 6.04. Found: C, 51.97; H, 4.96; N, 6.03%. IR: $\nu_{C=N}$ 1599 cm^{-1}.

*2.2.1.5. $[FeCl(5\text{-}MeOhapen)]\cdot 0.5MeOH$ **2′**.* Precursor complex **2′** was obtained as a black crystalline material by a similar method to that used in the preparation of **1′**, using H_2(5-MeOhapen) instead of H_2(4-MeOhapen). The product was obtained as black crystals. Yield: 3.84 g (86%). Found: C, 53.13; H, 5.08; N, 6.24%. Calcd. for $[FeCl(5\text{-}MeOhapen)]\cdot 0.5MeOH$ ($C_{20}H_{24}N_2O_4FeCl\cdot 0.5MeOH$): C, 53.33; H, 5.24; N, 6.07%. IR: $\nu_{C=N}$ 1614 cm^{-1}.

*2.2.1.6. $[FeCl(6\text{-}MeOhapen)]\cdot 0.25EtOH$ **3′**.* The precursor complex **3′** was obtained as a black crystalline material by a similar method to that used in the preparation of **1′**, using H_2(6-MeOhapen) and ethanol instead of H_2(4-MeOhapen) and methanol. The product

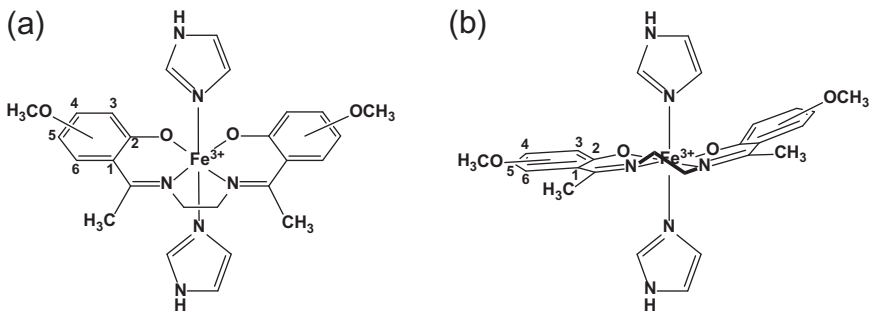

Scheme 1. (a) $[Fe^{III}(Him)_2(n\text{-}MeOhapen)]^+$ (**1**: $n = 4$, **2**: $n = 5$, **3**: $n = 6$). (b) Favorable conformation of two phenylidene planes for SCO.

was obtained as black crystals. Yield: 3.65 g (81%). *Anal.* Calc. for [FeCl(6-MeOhapen)]·0.25EtOH ($C_{20}H_{24}N_2O_4FeCl$·0.25EtOH): C, 53.85; H, 5.18; N, 6.13. Found: C, 54.09; H, 5.46; N, 6.23%. IR: $\nu_{C=N}$ 1591 cm^{-1}.

2.2.2. Preparation of iron(III) complex [$Fe^{III}(Him)_2$(n-MeOhapen)]PF_6·solvents

*2.2.2.1. [$Fe^{III}(Him)_2$(4-MeOhapen)]PF_6 (**1**).* To a suspension of [Fe^{III}Cl(4-MeOhapen)]·H_2O (0.5 mmol, 0.22 g) in 10 mL of methanol, an excess of imidazole (5 mmol, 0.34 g) was added, and the mixture was stirred for 30 min on a hot-plate at 65 °C and subsequently filtered. A solution of $NaPF_6$ (0.5 mmol, 0.09 g) in 5 mL of methanol was added to the filtrate, and the resulting solution was stirred for 15 min subsequently filtered. The resulting filtrate was allowed to stand for several hours, during which time black plate crystals precipitated; the crystals were collected by suction filtration, washed with diethyl ether, and dried in air. Yield: 0.23 g (67%). *Anal.* Calc. for [$Fe^{III}(Him)_2$(4-MeOhapen)]PF_6 ($C_{26}H_{30}N_6O_4FePF_6$): C, 45.17; H, 4.37; N, 12.15. Found: C, 45.15; H, 4.68; N, 12.21%. IR: $\nu_{C=N}$ 1606 cm^{-1}, ν_{N-H} 3419 cm^{-1}, ν_{P-F} 821 cm^{-1}. Thermogravimetric analysis (TGA) was carried out between room temperature and 145 °C using ca. 2 mg of the fresh crystalline sample: In the heating mode, a 0.8% weight loss was observed. In the cooling mode, the sample absorbed vapor to exhibit a 0.8% weight increase.

*2.2.2.2. [$Fe^{III}(Him)_2$(5-MeOhapen)]PF_6·0.5H_2O (**2**).* Compound **2** was prepared using a similar method to that used in the preparation of **1**, using [Fe^{III}Cl(5-MeOhapen)]·0.5MeOH instead of [Fe^{III}Cl(4-MeOhapen)]·H_2O. Black plate crystals were obtained as the product. Yield: 0.20 g (57%). *Anal.* Calcd. for [$Fe^{III}(Him)_2$(5-MeOhapen)]PF_6·0.5H_2O ($C_{26}H_{30}N_6O_4FePF_6$·0.5H_2O): C, 44.58; H, 4.46; N, 12.00. Found: C, 44.87; H, 4.42; N, 12.03%. IR: $\nu_{C=N}$ 1589 cm^{-1}, ν_{N-H} 3398 cm^{-1}, ν_{P-F} 817 cm^{-1}. TGA results of fresh crystalline sample: In the heating mode, a 2.1% weight loss was observed. In the cooling mode, the sample absorbed the vapor and exhibited a 1.0% weight increase.

*2.2.2.3. [$Fe^{III}(Him)_2$(6-MeOhapen)]PF_6·EtOH (**3**).* Compound **3** was prepared using a similar method to that used in the preparation of **1**, using [Fe^{III}Cl(6-MeOhapen)]·0.25EtOH and ethanol instead of [Fe^{III}Cl(4-MeOhapen)]·H_2O and methanol. Black plate crystals were obtained as the product. Yield: 0.24 g (66%). *Anal.* Calc. for [$Fe^{III}(Him)_2$(6-MeOhapen)]PF_6·EtOH ($C_{26}H_{30}N_6O_4Fe$-PF_6·EtOH): C, 45.60; H, 4.92; N, 11.39. Found: C, 45.71; H, 4.53; N, 11.58%. IR: $\nu_{C=N}$ 1586 cm^{-1}, ν_{N-H} 3397 cm^{-1}, ν_{P-F} 825 cm^{-1}. TGA results of fresh crystalline sample: In the heating mode, a 10.3% weight loss was observed. In the cooling mode, a weight increase was not observed.

2.3. Physical measurements

Elemental analyses (C, H, and N) were carried out at the Center for Instrumental Analysis of Kumamoto University. Melting points were measured by Yanako New Science Micro Melting Point System MP-S3. ^{1}H NMR spectra were measured by on a Varian ^{Unity}Inova AS400 with a static magnetic field of 9.4 T. Infrared spectra were recorded at room temperature using a PerkinElmer Frontier spectrometer with samples on ZnSe crystals. Thermogravimetric analysis (TGA) was carried out on a TG/DTA6200 (Seiko Instrument Inc.) instrument at a heating rate of 5 K min^{-1} using ca. 5 mg samples. Magnetic susceptibilities were measured by a Quantum Design MPMS-XL5 magnetometer in the temperature range of 5–300 K at a sweep rate of 2 K min^{-1} under an applied magnetic field of 0.5 T. The calibration was performed using palladium metal. Corrections for diamagnetism were applied using Pascal's constants [14].

2.4. Crystallographic data collection and structure analyses

X-ray diffraction data were collected on a Rigaku RAXIS RAPID imaging plate diffractometer using graphite monochromated Mo Kα radiation (λ = 0.71073 Å). The temperature of the crystal was maintained by a Rigaku cooling device within an accuracy of ±2 K. The data were corrected for Lorentz, polarization, and absorption effects. The structures were solved by a direct method, and expanded using the Fourier technique. Hydrogen atoms were fixed at the calculated positions and refined using a riding model. All calculations were performed using the CRYSTALSTRUCTURE crystallographic software package [15].

3. Results and discussion

3.1. Synthesis and characterization of iron(III) complexes [$Fe^{III}(Him)_2$(n-MeOhapen)]PF_6·solvents

The Fe^{III} complexes [$Fe^{III}(Him)_2$(n-MeOhapen)]PF_6·solvents (**1**: n = 4, **2**: n = 5, **3**: n = 6) were obtained as black plate crystals by mixing [Fe^{III}Cl(n-MeOhapen)], imidazole, and $NaPF_6$ in a 1:10:1 molar ratio in methanol for **1** and **2**, and in ethanol for **3**. The C, H, and N elemental analysis of complex **1** agreed with the formula [$Fe^{III}(Him)_2$(4-MeOhapen)]PF_6, demonstrating no existence of any crystal solvents. With **1**, the very gradual weight loss (within 0.1%) was observed in the heating mode in TGA. The elemental analysis of **2** agreed with the formula [$Fe^{III}(Him)_2$(5-MeOhapen)]PF_6·0.5H_2O. In the TGA, a 2.1% weight loss (0.8H_2O) was observed in the heating mode followed by a 1.1% weight increase (0.4 H_2O) in the cooling mode. The elemental analysis of **3** agreed with the formula [$Fe^{III}(Him)_2$(6-MeOhapen)]PF_6·EtOH. In TGA, a 6.4% weight loss (1EtOH) was observed in the heating mode and no weight increase was observed in the cooling mode.

The ethanolic solutions of all complexes are shown in Fig. 1(a). In the liquid state, **1** and **2** exhibited thermochromism, but **3** did not. The ethanolic solution of **1** was a deep red color at room temperature, and changed to a bluish-green color at liquid-nitrogen temperature. The ethanolic solution **2** was a violet color at room temperature, and changed to an olive-green color at

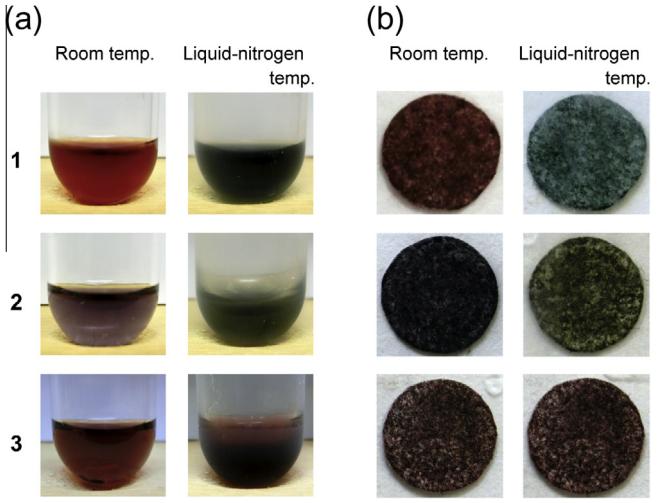

Fig. 1. (a) Thermochromism in ethanolic solutions of [$Fe^{III}(Him)_2$(n-MeOhapen)]PF_6·solvents. (**1**: n = 4, **2**: n = 5, **3**: n = 6) (b) thermochromism in the solid state of [$Fe^{III}(Him)_2$(n-MeOhapen)]-PF_6·solvents.

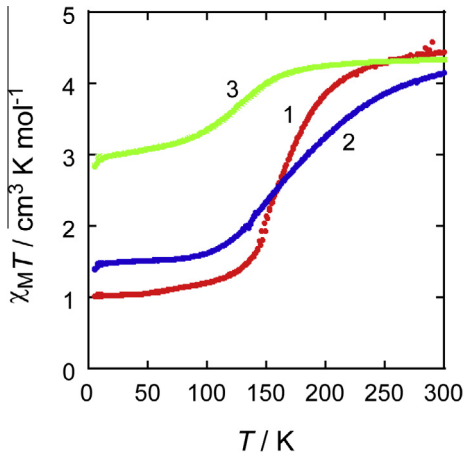

Fig. 2. $\chi_M T$ vs. T plots for **1**, **2**, and **3**.

liquid-nitrogen temperature. The ethanolic solution of **3** was a yellowish-brown color at room temperature did not show a color change upon decreasing the temperature. The thermochromism in the liquid state suggests SCO properties of isolated molecules. The color of the ground sample of all complexes are shown in Fig. 1(b). In the solid state, **1** and **2** showed thermochromism, but **3** did not. The color changes upon decreasing the temperature from room temperature to liquid-nitrogen temperature were similar to those of the ethanolic solutions. The thermochromism observed in the solid state suggests SCO properties of the crystal state.

3.2. Temperature-dependence of magnetic properties

The magnetic susceptibilities of the samples were measured in the temperature range of 5–300 K under an applied magnetic field of 0.5 T. The magnetic susceptibility was measured upon lowering the temperature from 300 to 5 K in the first run and was subsequently measured while raising the temperature in the second run. The $\chi_M T$ vs. T plots for **1**, **2**, and **3** are shown in Fig. 2. The plots of the data obtained in the heating and cooling modes were practically the same for the three complexes, and showed no thermal hysteresis.

Complex **1** showed a spin equilibrium between the HS and LS states. The $\chi_M T$ curves in warming and cooling modes showed a small difference in the spin transition temperature around 150 K. The $\chi_M T$ value of **1** was 4.5 cm^3 mol^{-1} K at 300 K, which was slightly higher than 4.375 cm^3 mol^{-1} K of the spin-only HS value. Upon decreasing the temperature from 300 K to 5 K, the $\chi_M T$ value decreased and then reached a constant value of ca. 1.0 cm^3 mol^{-1} K at 5 K, but was larger than 0.375 cm^3 mol^{-1} K of the spin-only LS value. Compound **2** showed a more gradual spin equilibrium than that of **1**. The $\chi_M T$ value of **2** was 4.1 cm^3 mol^{-1} K at 300 K, which was slightly lower than the spin-only HS value. Upon decreasing the temperature, the $\chi_M T$ value decreased gradually to 1.4 cm^3 mol^{-1} K at 5 K, but was considerably larger than the LS value. Compound **3** showed an incomplete spin equilibrium. The $\chi_M T$ value of **3** was 4.3 cm^3 mol^{-1} K at 300 K, which was comparable to the spin-only HS value. Upon decreasing the temperature, the $\chi_M T$ value decreased gradually to 2.8 cm^3 mol^{-1} K at 5 K, but was considerably larger than the LS value.

3.3. Crystal structures

3.3.1. Crystal structures of *1*, *2*, and *3*

The crystal structures of **1**, **2**, and **3** were determined by single-crystal X-ray diffraction analysis at various temperatures. The crystallographic data are listed in Table 1. Relevant coordination bond distances, angles, and hydrogen-bond distances are given in Table 2. The molecular structures of the $[Fe^{III}(Him)_2(n\text{-MeOhapen})]^+$ part and the atom numbering scheme of all complexes are shown in Figs. 3(a)–(c), in which the molecular structures projected on the Schiff-base planes and the side views are shown on the left and right side, respectively. Each Fe^{III} ion had an octahedral coordination environment with N_2O_2 donor atoms of the tetradentate Schiff-base ligand at the equatorial plane and N_2 donors of two imidazoles at the axial positions. The spin state of similar $[Fe^{III}(X)_2(salen\text{-}type)]^+$ systems (salen-type = salen-type N_2O_2 Schiff-base ligand; X = pyridine or imidazole) was explained by structural parameters. The coordination bond distances and angles are relevant parameters for the spin state. The Fe–N coordination bond distances of **1** and **2** at 296 K were in the range of those reported for HS Fe^{III} complexes with similar Schiff-base ligands [10–12]. The corresponding distances of **1** and **2** at 100 K were in the range of those reported for LS Fe^{III} complexes [10–12], and shorter than those at 296 K. The Fe–N distances of **3** were similar at 296 and 100 K, and were in the expected range for HS state Fe^{III} complexes. The O1–Fe–O2 bond angle is indicative of the spin state; the values of **1** and **2** at 296 K were 98.90(14)° for **1** and 98.10(17)° for **2**; these values were in the range of expected

Table 1
Crystallographic data for $[FeIII(Him)_2(n\text{-MeOhapen})]PF_6$·solvents (**1**: $n = 4$, **2**: $n = 5$, **3**: $n = 6$).

	[Fe(4-MeOhapen)]PF_6 (**1**)			[Fe(5-MeOhapen)]PF_6·H_2O (**2**)		[Fe(6-MeOhapen)]PF_6·EtOH (**3**)	
Formula	$C_{26}H_{30}N_6O_4FePF_6$			$C_{26}H_{30}N_6O_4FePF_6$·H_2O		$C_{26}H_{30}N_6O_4FePF_6$·C_2H_5OH	
Formula weight	691.37			709.39		737.44	
Crystal system	monoclinic	monoclinic	monoclinic	monoclinic	monoclinic	monoclinic	monoclinic
Space group	$C2/c$	$C2/c$	$C2/c$	$P2_1/n$	$P2_1/n$	$P\bar{1}$	$P\bar{1}$
T (K)	250	170	100	296	100	250	100
a (Å)	20.0759(5)	19.8295(6)	19.622(2)	11.0207(5)	10.8257(6)	10.1273(4)	10.0342(4)
b (Å)	17.1908(6)	17.0362(7)	16.912(2)	13.9014(6)	17.8663(9)	12.7833(5)	12.6380(5)
c (Å)	18.4139(5)	18.3305(6)	18.242(2)	19.875(1)	19.311(1)	15.1387(7)	15.0402(7)
α (°)	90	90	90	90	90	70.303(2)	70.638(2)
β (°)	112.3140(7)	111.7182(8)	111.354(2)	98.420(2)	98.986(2)	80.113(2)	80.499(1)
γ (°)	90	90	90	90	90	64.9446(9)	64.7394(9)
V (Å^3)	5879.1(3)	5752.9(4)	5638.0(8)	3012.2(3)	2863.2(3)	1670.6(1)	1626.7(1)
Z	8	8	8	4	4	2	2
$D_{calc.}$ (g cm^{-3})	1.562	1.596	1.629	1.564	1.646	1.466	1.505
μ (cm^{-1})	6.491	6.633	6.768	6.379	6.711	5.781	5.937
R[a]	0.0590	0.0609	0.1274	0.0759	0.1246	0.1027	0.0379
Rw[b]	0.1838	0.1865	0.3554	0.2148	0.3388	0.3086	0.1515

[a] $R = \Sigma||Fo| - |Fc||/\Sigma|Fo|$.
[b] $Rw = [\Sigma w(|Fo^2| - |Fc^2|)^2/\Sigma w|Fo^2|^2]^{1/2}$.

Table 2
Coordination bond distances (Å), bond angles (°) and Hydrogen bond distances (Å) for $[Fe^{III}(Him)_2(n\text{-}MeOhapen)]PF_6 \cdot solvents$ (**1**: $n = 4$, **2**: $n = 5$, **3**: $n = 6$).

	[Fe(4-MeOhapen)]PF_6 (**1**)			[Fe(5-MeOhapen)]$PF_6 \cdot H_2O$ (**2**)		[Fe(6-MeOhapen)]$PF_6 \cdot$EtOH (**3**)	
	250 K	170 K	100 K	296 K	100 K	250 K	100 K
Bond lengths (Å)							
Fe–N1	2.093(3)	2.015(3)	1.945(6)	2.073(5)	1.938(8)	2.105(4)	2.1133(15)
Fe–N2	2.072(4)	1.998(4)	1.937(8)	2.085(5)	1.928(7)	2.104(6)	2.103(3)
Fe–N3	2.173(5)	2.089(5)	2.013(9)	2.133(6)	1.980(9)	2.169(4)	2.1434(16)
Fe–N5	2.164(5)	2.078(5)	2.023(9)	2.129(6)	2.000(8)	2.144(4)	2.1590(16)
Average <Fe–N>	2.125	2.045	1.980	2.105	1.962	2.131	2.1297
Fe–O1	1.875(4)	1.881(4)	1.875(7)	1.885(4)	1.893(6)	1.893(5)	1.8859(19)
Fe–O2	1.883(3)	1.882(3)	1.884(5)	1.882(4)	1.870(6)	1.918(4)	1.9293(14)
Average <Fe–O>	1.879	1.881	1.879	1.883	1.881	1.906	1.908
Bond angles (°)							
O1–Fe–O2	98.90(14)	93.30(13)	88.6(3)	98.10(17)	86.3(3)	104.36(17)	103.90(7)
O1–Fe–N1	88.63(15)	90.83(14)	92.2(3)	90.44(18)	94.0(3)	87.97(18)	88.51(7)
O2–Fe–N2	90.73(14)	92.16(13)	94.1(3)	88.91(18)	93.4(3)	87.38(18)	87.23(7)
N1–Fe–N2	81.88(15)	83.83(13)	85.2(3)	82.55(19)	86.3(3)	80.53(18)	80.60(6)
N1–Fe–N3	90.67(15)	91.40(14)	92.4(3)	87.40(19)	89.5(4)	88.53(14)	87.44(6)
N1–Fe–N5	88.08(15)	88.56(14)	89.5(3)	88.90(20)	91.9(4)	87.18(14)	86.87(6)
N2–Fe–N3	88.07(18)	88.80(16)	90.4(4)	89.60(20)	91.4(4)	88.76(18)	89.24(7)
N2–Fe–N5	89.12(16)	90.39(15)	91.8(4)	89.00(19)	91.7(3)	87.89(18)	87.55(7)
Hydrogen bond distances (Å)							
N4H···F1[a] (or O5[b,c])	2.920(9)	2.921(6)	2.914(15)	2.862(16)	2.82(3)	2.761(7)	2.744(3)
N6H···F3[a] (or O1[b])	3.059(8)	3.047(6)	3.029(12)	2.949(7)	2.850(10)		
O5H···O2						2.759(9)	2.751(3)

[a] [Fe(4-MeOhapen)]PF_6 (**1**).
[b] [Fe(5-MeOhapen)]$PF_6 \cdot H_2O$ (**2**).
[c] [Fe(6-MeOhapen)]$PF_6 \cdot$EtOH (**3**).

values for HS Fe^{III} complexes [10–12]. The corresponding angles of **1** and **2** at 100 K were 88.6(3)° and 86.3(3)°, respectively, whose values are closer to those of a regular octahedron than those at 296 K. The O1–Fe–O2 angles of **3** were 104.36(17)° at 296 and 104.36(17)° at 100 K, but were much distorted than those of **1** and **2**.

Fig. 3 (left side) shows the orientations of the two imidazole rings in the compounds. For **1** and **3**, the two imidazole rings were oriented nearly along the two N–Fe–O diagonals. For **2**, one imidazole ring bisected the angles defined by the two N–Fe–O diagonals, and the other imidazole ring was oriented nearly along the N–Fe–O diagonal. Fig. 3 (right side) shows the side view of the

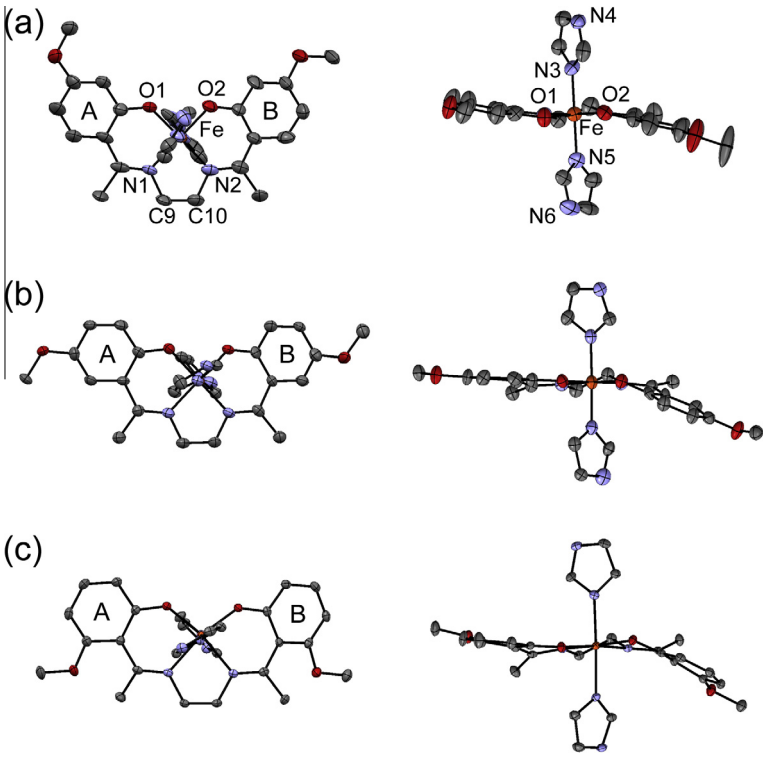

Fig. 3. (a) (left side) Side view of the complex-cation. The thermal ellipsoids were drawn at the 50% probability level. (right side) ORTEP drawing of $[Fe^{III}(Him)_2(4\text{-}MeOhapen)]^+$ of **1** projected on the planar Schiff-base ligand with the selected atom numbering scheme at 100 K. (b) The molecular structures of **2**. (c) The molecular structure of **3** at 100 K.

complex-cation. In all three complexes, the saturated five-membered chelate ring involving the ethylenediamine moiety adopted the gauche conformation, in which two carbon atoms deviated at opposite positions from the plane defined by FeN_2 in all three complexes and at all temperatures. Murray et al. demonstrated that the five-membered chelate ring FeC_2N_2 is closely related to the spin state, as the envelope conformation allows the spin transition, and the gauche or planar conformation locks in high spin state [11]. As demonstrated above, complexes **1**–**3** have gauche conformation, but the phenylidene planes were oriented opposite to the FeO_2N_2 coordination plane. For example, the deviated distances of C9 and C10 atoms from the FeN_2 plane for **1** at 100 K were +0.279 and −0.265 Å, respectively (+0.180 and −0.441 Å for **2**, +0.194 and −0.495 Å for **3**). The dihedral angles of the benzene rings A and B from the FeN_2O_2 plane for **1** were +14.56° and −14.86°, respectively (+3.62° and −25.77° for **2**, +10.04° and −31.02° for **3**). Benzene ring B was increasingly tilted from the coordination plane in the following order: **1** < **2** < **3**, suggesting that the tilting of the benzene rings occurs due to the steric hindrance between the methyl and n-methoxy group at the phenylidene moiety. Complexes **1** and **2** with n-methoxy groups (n = 4 and 5) may have a flexible conformation and may be suitable for a structural change from the HS to LS spin transition due to the small steric hindrance. The large steric hindrance observed in **3** with the 6-methoxy group may lock the N_2O_2 ligand conformation.

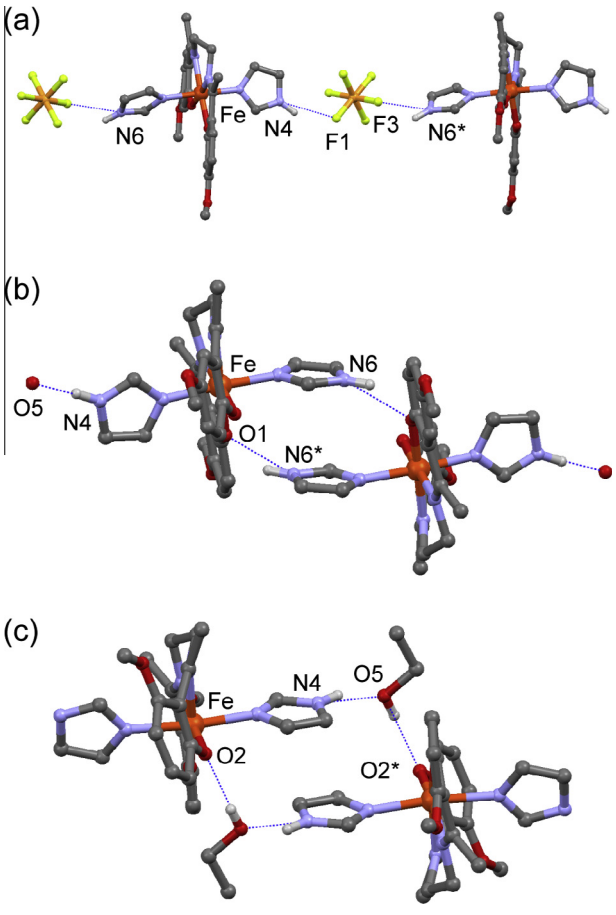

Fig. 4. (a) 1D structure by hydrogen bonds between PF_6^- and imidazole of **1**, $\{\cdots[Fe(Him)_2(4\text{-MeOhapen})]^+\cdots PF_6^-\cdots\}_\infty$. (b) Cyclic dimer structure constructed by hydrogen bond of imidazole…phenoxo oxygen of **2**, $\{\cdots[Fe(Him)_2(5\text{-MeOhapen})]^+\cdots\}_2$. (c) Cyclic dimer structure constructed from hydrogen-bonds through ethanol of **3**, $\{\cdots[Fe(Him)_2(6\text{-MeOhapen})]^+\cdots EtOH\cdots\}_2$. The structures of **2** and **3** have an inversion center.

3.3.2. Three types of hydrogen-bonded assembly structures

Fig. 4(a)–(c) shows the assembly structures of **1**, **2**, and **3**, respectively. Complex **1** contained one-dimensional (1D) chain structures. The 1D structure of **1** was composed of weak hydrogen bonds between the imidazole nitrogen and PF_6^- ion. Specifically, one PF_6^- anion bridges two adjacent $[Fe^{III}(Him)_2(4\text{-MeOhapen})]^+$ cations with hydrogen bonds of F(1)···N(4) and F(3)···N(6)*. The adjacent cations are related by a two-fold screw axis along the *b*-axis to form a 1D structure. In the crystal lattice, rods are stacked along the *b*-axis, and the anions occupy the space among the rods.

Fig. 4(b) and (c) shows the two cyclic dimer structures of **2** and **3**. Both cyclic dimer structures had an inversion center and the PF_6^- ion was not involved in the cyclic dimer structure. In complex **2**, one of the two imidazoles was hydrogen bonded to one of two phenoxo oxygen atoms of the adjacent complex-cation with N(6)···O(1)* to form a cyclic dimeric structure, $\{\cdots[Fe^{III}(Him)_2(5\text{-MeOhapen})]\cdots\}_2$, while the other imidazole N(4) is hydrogen bonded to a water molecule. In complex **3**, one of the two imidazoles is hydrogen bonded to the oxygen atom O(5) of ethanol with N(4)···O(5), while the other imidazole does not form any hydrogen bonds. The oxygen atom O(5) is also hydrogen bonded to one of two phenoxo oxygen atoms of the adjacent complex-cation with O(5)···O(2) to form a cyclic dimer structure, $\{\cdots[Fe^{III}(Him)_2(hapen)]\cdots(EtOH)\cdots\}_2$.

4. Concluding remarks

Three Fe^{III} complexes $[Fe^{III}(Him)_2(n\text{-MeOhapen})]PF_6$ solvents (**1**: n = 4, **2**: n = 5, **3**: n = 6) with three isomers of the new "hapen-type" ligand (n-MeOhapen) were synthesized. Three types of hydrogen-bonded assembly structures were generated, including a 1D chain in **1**, and a cyclic dimer in **2** and **3**, whose Fe^{III} ion was coordinated by N_4O_2 donor atoms of equatorial n-MeOhapen and two axial Him. The saturated FeC_2N_2 chelate ring involving the ethylenediamine moiety adopted a gauche conformation and the two phenylidene planes of $[Fe^{III}(Him)_2(n\text{-MeOhapen})]^+$ were oriented opposite to the FeO_2N_2 coordination plane, suggesting that the tilting of the phenylidene planes occurs due to the steric hindrance between the methyl and n-methoxy group at the phenylidene moiety. Complex **1** and **2** showed SCO behavior, but **3** showed incomplete SCO. The N_2O_2 conformation in **1** and **2** with n-methoxy groups (n = 4 and 5) may facilitate the structural change from the HS to LS spin transition due to the small steric hindrance. The ligand conformation in **3** with the 6-methoxy group may promote the HS state, due to the large steric hindrance. These results demonstrate that the conformation of the N_2O_2 Schiff-base ligand is related to SCO behavior of the complexes.

Acknowledgment

T. Fujinami was supported by the Research Fellowship for Young Scientists of the Japan Society for the Promotion of Science, KAKENHI 00248556.

Appendix A. Supplementary material

CCDC 1030202–1030208 contains the supplementary crystallographic data for $[Fe^{III}(Him)_2(4\text{-MeOhapen})]PF_6$ (**1**) at 100, 170 and 250 K, $[Fe^{III}(Him)_2(5\text{-MeOhapen})]PF_6{\cdot}H_2O$ (**2**) at 100 and 296 K, and $[Fe^{III}(Him)_2(6\text{-MeOhapen})]PF_6{\cdot}EtOH$ (**3**) at 100 and 250 K, respectively. These data can be obtained free of charge from The Cambridge Crystallographic Data Centre via www.ccdc.cam.ac.uk/data_request/cif. Supplementary data associated with this article can be found, in the online version, at http://dx.doi.org/10.1016/j.ica.2015.03.034.

References

[1] (a) P. Gütlich, H.A. Goodwin, Spin Crossover in Transition Metal Compounds I–III, Topics in Current Chemistry, Springer, New York, 2004. 233–235;
(b) J.A. Real, A.B. Gaspar, V. Niel, M.C. Muñoz, Dalton Trans. (2005) 2062.

[2] (a) T. Fukukai, K. Yabe, Y. Ogawa, N. Matsumoto, J. Mrozinski. Bull. Chem. Soc. Jpn. 78 (2005) 1484;
(b) K. Tanimura, R. Kitashima, N. Brefuel, M. Nakamura, N. Matsumoto, S. Shova, J.P. Tuchagues, Bull. Chem. Soc. Jpn. 78 (2005) 1279.

[3] Floquet Sébastien, Rivière Eric, Boukheddaden Kamel, Morineau Denis, Marie-Laure Boillot, Polyhedron 80 (2014) 60.

[4] T. Fujinami, M. Koike, N. Matsumoto, Y. Sunatsuki, A. Okazawa, N. Kojima, Inorg. Chem. 53 (2014) 2254.

[5] (a) B. Weber, W. Bauer, J. Obel, Angew. Chem., Int. Ed. 47 (2008) 10098;
(b) B. Weber, Coord. Chem. Rev. 253 (2009) 2432.

[6] (a) M. Yamada, H. Hagiwara, H. Torigoe, N. Matsumoto, M. Kojima, F. Dahan, J.P. Tuchagues, N. Re, S. Iijima, Chem. Eur. J. 12 (2006) 4536;
(b) Y. Ikuta, M. Ooidemizu, Y. Yamahata, M. Yamada, S. Osa, N. Matsumoto, S. Iijima, Y. Sunatsuki, M. Kojima, F. Dahan, J.P. Tuchagues, Inorg. Chem. 42 (2003) 7001;
(c) T. Sato, K. Nishi, S. Iijima, M. Kojima, N. Matsumoto, Inorg. Chem. 48 (2009) 7211;
(d) T. Buchen, P. Gütlich, K.H. Sugiyarto, H.A. Goodwin, Chem. Eur. J. 2 (1996) 1134;
(e) K.H. Sugiyarto, M.L. Scudder, D.C. Craig, H.A. Goodwin, Aust. J. Chem. 53 (2000) 755;
(f) Y. Sunatsuki, Y. Ikuta, N. Matsumoto, H. Ohta, M. Kojima, S. Iijima, S. Hayami, Y. Maeda, S. Kaizaki, F. Dahan, J.P. Tuchagues, Angew. Chem., Int. Ed. 42 (2003) 1614;
(g) T. Fujinami, K. Nishi, N. Matsumoto, S. Iijima, M.A. Halcrow, Y. Sunatsuki, M. Kojima, Dalton Trans. 40 (2011) 12301;
(h) K. Nishi, N. Matsumoto, S. Iijima, M.A. Halcrow, Y. Sunatsuki, M. Kojima, Inorg. Chem. 50 (2011) 11303;
(i) D. Furushou, T. Hashibe, T. Fujinami, K. Nishi, H. Hagiwara, N. Matsumoto, Y. Sunatsuki, M. Kojima, S. Iijima, Polyhedron 44 (2012) 194.

[7] (a) A.H. Ewald, R.L. Martin, I.G. Ross, A.H. White, Proc. R. Soc. A280 (1984) 235;
(b) G. Harris, Theoret. Chim. Acta 5 (1966) 379;
(c) M. Zerner, M. Gouterman, H. Kobayashi, Theor. Chim. Acta 6 (1966) 363.

[8] (a) J.P. Collman, T.N. Sorrell, K.O. Hodgson, A.K. Kulshrestha, C.E. Strouse, J. Am. Chem. Soc. 99 (1977) 5180;
(b) J.P. Collman, X. Zhang, K. Wong, J.I. Brauman, J. Am. Chem. Soc. 116 (1994) 6245;
(c) D.H. Busch, N.W. Alcock, Chem. Rev. 94 (1994) 585;
(d) W.R. Scheidt, J. Am. Chem. Soc. 105 (1983) 2625;
(e) D.K. Geiger, Y.J. Lee, W.R. Scheidt, J. Am. Chem. Soc. 106 (1984) 6339.

[9] (a) Y. Nishida, S. Oshio, S. Kida, Chem. Lett. (1975) 79;
(b) Y. Nishida, S. Oshio, S. Kida, Bull. Chem. Soc. Jpn. 50 (1977) 119;
(c) Y. Nishida, K. Kino, S. Kida, J. Chem. Soc., Dalton Trans. (1987) 1157.

[10] (a) N. Matsumoto, K. Kimoto, A. Ohyoshi, Y. Maeda, Chem. Lett. (1984) 479;
(b) N. Matsumoto, K. Kimoto, A. Ohyoshi, Y. Maeda, Bull. Chem. Soc. Jpn. 57 (1984) 3307;
(c) Y. Maeda, Y. Takashima, N. Matsumoto, A. Ohyoshi, J. Chem. Soc., Dalton Trans. (1986) 1115;
(d) M. Koike, K. Murakami, T. Fujinami, K. Nishi, N. Matsumoto, Y. Sunatsuki, Inorg. Chim. Acta 399 (2013) 185.

[11] (a) B.J. Kennedy, A.C. McGrath, K.S. Murray, B.W. Skelton, A.H. White, Inorg. Chem. 26 (1987) 483;
(b) T.M. Ross, S.M. Neville, D.S. Innes, D.R. Turner, B. Moubaraki, K.S. Murray, J. Chem. Soc., Dalton Trans. 39 (2010) 149.

[12] R. Hernandenz-Molina, A. Mederos, S. Dominguez, P. Gili, C. Ruiz-Perez, A. Castineiras, X. Solans, F. Lloret, J.A. Real, Inorg. Chem. 37 (1998) 5102.

[13] T.D. Roberts, M.A. Little, L.J. Kershaw, Dalton Trans. 43 (2014) 7577;
P. Masárová, P. Zoufalý, J. Moncol, I. Nemec, J. Pavlik, M. Gembický, Z. Trávníček, New J. Chem. 39 (2015) 508.

[14] O. Kahn, Molecular Magnetism, VCH, Weinheim, Germany, 1993.

[15] CrystalStructure 4.0: Crystal Structure Analysis Package, Rigaku Corporation (2000–2010), Tokyo, Japan.